MRI study of the changes in crystalline lens shape with accommodation and aging in humans

Sanjeev Kasthurirangan

School of Optometry and Institute of Health & Biomedical Innovation, Queensland University of Technology, Brisbane, Q, AUSTRALIA

* Currently employed with ABBOTT Medical Optics Milpitas, CA, USA

Emma L. Markwell

School of Optometry and Institute of Health & Biomedical Innovation, Queensland University of Technology, Brisbane, Q, AUSTRALIA

David A. Atchison

School of Optometry and Institute of Health & Biomedical Innovation, Queensland University of Technology, Brisbane, Q, AUSTRALIA

James M. Pope

Physics, Faculty of Science & Technology and Institute of Health & Biomedical Innovation, Queensland University of Technology, Brisbane, Q, AUSTRALIA

Abstract

Magnetic Resonance Imaging was used to study changes in the crystalline lens and ciliary body with accommodation and aging. Monocular images were obtained in 15 young (19-29 years) and 15 older (60-70 years) emmetropes when viewing at far (6m) and at individual near points (14.5 to 20.9 cm) in the younger group. With accommodation, lens thickness increased (mean±95% CI: 0.33±0.06mm) by a similar magnitude to the decrease in anterior chamber depth (0.31±0.07mm) and equatorial diameter (0.32±0.04mm) with a decrease in the radius of curvature of the posterior lens surface (0.58±0.30mm). Anterior lens surface shape could not be determined due to the overlapping region with the iris. Ciliary ring diameter decreased (0.44±0.17mm) with no decrease in circumlental space or forward ciliary body movement. With aging, lens thickness increased (mean±95% CI: 0.97±0.24mm) similar in magnitude to the sum of the decrease in anterior chamber depth (0.45±0.21mm) and increase in anterior segment depth (0.52±0.23mm). Equatorial lens diameter increased (0.28±0.23mm) with no change in the posterior lens surface radius of curvature. Ciliary ring diameter decreased (0.57±0.41mm) with reduced circumlental space (0.43±0.15mm) and no forward ciliary body movement. Accommodative changes support the Helmholtz theory of accommodation including an increase in posterior lens surface curvature. Certain aspects of aging changes mimic accommodation.

Keywords: Presbyopia, mechanism of accommodation, anterior chamber depth, anterior segment length, asphericity, lens, lens thickness, ocular parameters, radius of curvature, equatorial diameter, cataract surgery, accommodation restoration.

Introduction

Ocular accommodation is a change in the optical power of the eye with an attempt to focus at near. Accommodation occurs by ciliary muscle contraction which leads to changes in the shape of the crystalline lens (Glasser & Kaufman, 1999; Helmholtz von, 1924). With increasing age, it is generally believed that the crystalline lens progressively loses elasticity, leading to a complete inability to change shape and to loss of accommodation by the mid fifties (Atchison, 1995; Duane, 1912). The loss in near visual function associated with the loss in accommodation is termed '*presbyopia*'. Much of the recent research on the accommodative mechanism of the eye has been prompted by interest in the restoration of accommodation in presbyopes. In theory, accommodation can be restored surgically by replacing the inelastic crystalline lens with an elastic material, by laser assisted intra-lenticular photodisruption to restore elasticity or by replacing the crystalline lens with an "accommodating" IOL (Nishi, Hara, Sakka, Hayashi, Nakamae & Yamada, 1992; Parel, Gelender, Trefers, & Norton, 1986; Krueger, Sun, Stroh, & Myers, 2001; Dick, 2005). Current approved techniques for restoring accommodation involve implantation of an accommodating intraocular lens (AIOL) during cataract surgery eg: Crystalens (Bausch & Lomb, USA) and 1CU (Humanoptics AG, Germany). These IOLs have been shown to restore only up to 1 D of accommodation (Mastropasqua, Toto, Nubile, Falconio, & Ballone, 2003; Cumming, Slade, & Chayet, 2001). The relatively modest effect is due in part to physiological and theoretical limits of performance i.e. the limited (~1 D) dioptric power change per millimeter movement of a single optic lens (Dick, 2005; Ho, Manns, Pham, & Parel, 2006). Other methods of restoring larger amounts of accommodation being developed include novel IOLs (Synchrony Dual Optic IOL, Abbott Medical Optics, USA; NuLens, NuLens Ltd., Israel and PowerVision IOL, PowerVision Inc., USA), polymer refilling of the capsular bag (Koopmans, Terwee, Barkhof, Haitjema, & Kooijman, 2003; Koopmans, et al., 2006) and extra-lenticular surgical procedures to increase the space between ciliary muscle and crystalline lens (Priavision Inc., USA). Currently only limited restoration of accommodation following cataract surgery has been achieved, while the ultimate goal of restoring large amounts of accommodation in presbyopes without cataract (i.e. through clear lens extraction) is yet to be realized. A better understanding of the mechanism of accommodation and age-related changes in ocular structures involved in accommodation will help in developing and refining surgical procedures designed to restore accommodation in presbyopes.

The current study characterizes the changes in the shape of the crystalline lens and location of the ciliary body with accommodation and age in normal human subjects.

Most previous *in-vivo* studies on crystalline lens shape have utilized optical techniques such as catoptric and slit lamp imaging or ultrasound based imaging. Optical techniques have been employed to study the shape of the crystalline lens as visible through the pupil (Koretz, Bertasso, Neider, True-Gabelt, & Kaufman, 1987; Rosales & Marcos, 2006; Dubbelman & Van Der Heijde, 2001; Brown, 1973; Smith & Garner, 1996; Atchison, Markwell, Kasthurirangan, Pope, Smith, & Swann. 2008). Accurate characterization of lens thickness and posterior surface curvature using optical techniques could be influenced by changes in the anterior surface and refractive index distribution of the lens with accommodation and age (Dubbelman, Van Der Heijde, & Weeber, 2001). Ultrasound imaging techniques have been used for axial measurements of biometric distances within the eye and to image the lens periphery and ciliary body (Beers & Van Der Heijde, 1994; Ostrin & Glasser, 2007; Vilupuru & Glasser, 2003; Stachs, Martin, Kirchhoff, Joachim, Terwee, & Guthoff, 2002). The advantages of ultrasound based techniques are images not affected by refractive effects due to changes in crystalline lens shape with accommodation or aging, and the ability to image behind the iris. However, age-related variation in speed of sound in the crystalline lens is not fully understood (Atchison, et al., 2008; Beers & Van Der Heijde, 1994; Koretz, Kaufman, Neider, & Goeckner, 1989). Ultrasound techniques also usually lack internal references or landmarks unless tattoos are used, as in some animal studies (Ostrin & Glasser, 2007). Whole lens *in-vivo* imaging, including characterization of lens surfaces, has not been undertaken with optical (due to the presence of iris) or ultrasound (restricted field of view) techniques. In short, while past studies using optical or ultrasound techniques have provided reliable axial and central anterior lens surface characteristics, whole lens shapes including posterior surface characteristics have not been clearly described.

MRI is a non-optical imaging technique and does not require any assumptions concerning lens optical properties for dimensional measurements. Consequently accommodative and age-related changes in the optical properties of the crystalline lens are not expected to create any distortions in the MR images of the lens. However, MRI is a relatively time consuming technique and is of lower resolution compared to optical and ultrasound techniques. MRI has been used previously for ocular imaging to study overall eye shape, extraocular muscle anatomy, crystalline lens shape, refractive index distribution and ciliary muscle anatomy (Atchison & Smith, 2004; Demer, Clark, Crane, Tian, Narasimhan & Karim, 2008; Atchison,

et al., 2008; Jones, Atchison, & Pope, 2007; Strenk, Strenk, Semmlow, & DeMarco, 2004; Jones, et al., 2007; Kasthurirangan, Markwell, Atchison, & Pope, 2008; Strenk, Strenk, & Semmlow, 2000). We have previously described the dependence of refractive index distribution of the crystalline lens on accommodation and age using MRI imaging (Jones, et al., 2007; Kasthurirangan, et al, 2008). Strenk et al reported anterior chamber depth, crystalline lens diameter, thickness and surface area and ciliary ring diameter as a function of age and accommodation using MRI (Strenk, Semmlow, Strenk, Munoz, Gronlund-Jacob, & DeMarco, 1999; Strenk, et al., 2000; Strenk, et al., 2004), but did not describe changes in curvature and shape of the lens surfaces with age and accommodation.

The aim of the current study was to use MRI to study changes in crystalline lens shape and ciliary body position with accommodation in 20 to 30 year old subjects, and with aging in 60 to 70 year old subjects. Some of the results on crystalline lens shape from the present study have been reported previously (Atchison, et al., 2008). The present report provides a complete description of the crystalline lens shape including previously unreported information on the asphericity of lens surfaces, measures of overall lens shape and ciliary body position.

Methods

Subjects

Subject demography and experimental set up are as described previously (Kasthurirangan, et al., 2008). Only a brief description of the methods is provided here. Fifteen young and fifteen older subjects were recruited. Young subjects were between 19 and 29 years (mean ± 1 SD: 22.8 ± 3.1 years) and older subjects were between 60 and 70 years (mean ± 1 SD: 64.3 ± 3.2 years). All subjects had good ocular and general health. A preliminary examination confirmed emmetropia (± 0.75 D sphere and ≤ 0.50 D cylinder) with 6/6 distance visual acuity in the tested eye. The research followed the tenets of the Declaration of Helsinki. The experimental protocol was approved by the Queensland University of Technology and Prince Charles Hospital human ethics review boards. Informed consent was obtained from all subjects.

MRI Technique

Monocular MR images were obtained with a General Electric "Twin Speed" clinical MR scanner operating at a field strength of 1.5 Tesla (Signa Twin Speed; GE Medical Systems, Milwaukee, WI). Subjects lay supine in the MR equipment with the head stabilized with foam pads (see Figure 1 of Kasthurirangan et al, 2008 for schematic of experimental set up). A 3.5 cm receive-only surface coil (Nova Medical, Wilmington MA) was used to obtain high resolution images from one eye of each subject in the transverse axial and sagittal planes. After obtaining a set of scout images to ensure eye alignment (see details in *Experimental Procedures* section), a Fast Spin Echo (FSE) imaging sequence was used to obtain high resolution images for dimensional measurements within the eye. MR images were acquired with a 40 mm field of view and 3 mm slice thickness, an effective echo time TE = 19 ms, an echo train length of 4, 320 × ×320 matrix size (interpolated to 512 × ×512 pixel images) and a recycle time TR = 400 ms, giving a total image acquisition time of 2 minutes and 11 seconds. During the same session another imaging sequence (Multi Spin Echo) was used for refractive index measurements as reported previously (Kasthurirangan, et al., 2008).

Experimental Procedures

In young subjects MRI measurements were performed for far and near viewing, while in the older subjects MRI measurements were performed only for far viewing. The MRI eye coil, with a viewing hole in the middle, was placed in front of and as close as possible to the measured eye (without touching the skin or eye lashes) and clamped in place. A mirror tilted vertically by 45° was placed 10 cm above the eye. The subject looked through the mirror at the center of a 31-mm-diameter spoke-wheel target on a wall 6.1 m away. The subject was instructed to look at the target during the measurements and to relax between measurements. The order of image acquisition was (1) a 16 second set of scout images, (2) an FSE image in the sagittal plane of the eye, (3) an FSE image in the transverse axial plane, (4) an MSE image in the sagittal plane and (5) an MSE image in the transverse axial plane. If the eye appeared tilted in the sagittal scout images, the vertical tilt of the mirror was adjusted appropriately and another set of scout images was obtained. The transverse axial scout images were used to manually select the slice plane for the first sagittal FSE image to correspond with the geometrical axis of the

crystalline lens. The sagittal FSE image was used to determine the slice for the next transverse axial FSE image i.e. in the sequence mentioned above, each image was used to set up the axis for the next image.

In young subjects, MR images during near viewing were obtained while fixating on a spoke-wheel target placed in a mount in front of and as close as possible to the eye, so that it could still be seen clearly and comfortably. The near target was removed from the mount to reveal a round hole in the mount. The subject was instructed to move the mount vertically and horizontally until the distant target appeared centered in the hole. The mount was locked in place, and the near target was replaced. In this manner, the near target was subjectively aligned with the distant target, to maintain similar gaze direction for far and near scans. The subject was instructed to look at the near target and keep it in focus. The range of near target distances for different subjects was 14.5 to 20.9 cm, which corresponds to 6.9 to 4.8 D of accommodative stimulus.

Data Analysis

The MR images were analyzed with custom written software in Matlab (The MathWorks Inc., Natick MA). MR images during far and near viewing for a young subject, and far viewing only for an older subject, are shown in Figure 1. External and internal boundaries in the eye were identified using a Canny edge filter available in Matlab Image Processing Toolbox. The eye image was rotated to orient vertically with cornea above and sclera below (Figure 1B). The angle of rotation was noted to check for any gaze deviations between far and near viewing in young subjects. Adequate performance of the eye rotation algorithm has been reported previously (Kasthurirangan, et al., 2008).

A difficulty in the identification of crystalline lens pixels is that the iris obscures part of the anterior edge of the lens. Therefore, the user manually defined two regions on either side of the pupil around the region of contact between the iris and the lens. These regions were removed from further analysis. The remaining anterior and all of the posterior edge data of the lens were individually smoothed with a conic curve (Dubbelman & Van Der Heijde, 2001):

$$y = \frac{c(x - x_0)^2}{1 + \sqrt{1 - kc^2(x - x_0)^2}} + y_0 \qquad (1)$$

where x_0, y_0 is the vertex position, c is the curvature at the vertex and k is the conic constant. This curve was used to obtain the curvature at vertex and the asphericity over 99% of the anterior (excluding iris-covered regions) and posterior surfaces of the lens.

Various biometric parameters were measured automatically from the MR images (see Figure 1B). These included 1. anterior chamber depth (ACD: distance from the front of the cornea to anterior pole of the crystalline lens), 2. lens axial thickness (LT: distance between anterior and posterior poles of the lens), 3. anterior segment depth (ASD: distance from the front of the cornea to the posterior pole of the lens), 4. lens equatorial diameter (ED: distance between the equatorial edges of the lens), 5. lens surface curvatures and asphericity (obtained from conic curve fits over 99% of anterior and posterior lens surfaces), 6. ratio of lens axial thickness to equatorial diameter as a metric of lens shape (LT/ED ratio), 7. ciliary ring diameter (distance between innermost ciliary body tips identified manually), 8. ciliary body depth (axial distance between anterior cornea and a line joining innermost ciliary body tips) and 9. axial length (distance between anterior cornea and posterior edge (outer sclera) of the eye – note that the retina was not always clearly visible in the MR images and so the posterior edge of the eye was used). Axial length was measured along a geometric axis of the eye (Figure 1B). All measurements, except for ciliary ring diameter, were automatically performed. Statistical comparisons for accommodative trends were performed through paired t-tests and for age-related trends through unpaired t-tests. An α level of 0.05 was considered to be significant.

Lens thickness and axial length measured with MRI during relaxed accommodation were compared with A-scan ultrasound (Axis-II A-scan, Quantel Medical Inc., USA) measurements during far fixation in the same eyes to evaluate the accuracy of MRI dimension measurements.

Results

Resolution and noise level

In general, the sagittal images were noisier than the transverse axial images. In order to quantitatively evaluate this difference, signal-to-noise ratio and the intensity gradient across the anterior edge of the crystalline lens were compared between sagittal and transverse axial images in the same eyes. Signal-to-noise ratio was calculated as the ratio of average pixel intensity within the crystalline lens (signal) and average pixel intensity anterior to the cornea (i.e. region with no ocular structures to calculate noise). The average signal-to-noise ratio was significantly larger in the transverse axial images than in the sagittal images (5.31 vs 4.81, paired t-test, $p < 0.01$). Peak intensity gradient across the crystalline lens was calculated in the following manner: (1) the intensity gradient along five lines of pixels across the anterior lens surface from the anterior chamber into the lens was calculated, (2) an average of peak intensity gradients from the five lines was calculated, and (3) average peak intensity gradient was considered as the intensity difference across the anterior lens surface. Average intensity gradient in the transverse axial images was 31% greater than in sagittal images (paired t-test, $p < 0.01$). The increased noise was mainly due to motion artifacts, most likely due to blinks, affecting the sagittal images more than the transverse axial images. Paired comparisons revealed statistically significant differences between sagittal and transverse axial images for some ocular biometric parameters. Since ocular measurements with transverse axial images show some differences from sagittal images and the transverse axial images were sharper with well defined edges compared to sagittal images, further results are presented for transverse axial data only.

The MR images had an in-plane resolution of 0.078 mm/pixel based on 40 mm field of view with image resolution of 512 x 512 pixels. Profile plots of intensity change along the anterior lens surface showed that the edge consisted of two pixels of rising intensity (or grey values). As an upper estimate, the uncertainty in defining a surface edge was of one pixel length, i.e. one of the two pixels could be determined as the edge. The error in measuring intra-ocular lengths (i.e. distance between two surfaces) was therefore two pixels (one pixel error for each surface) or 0.156 mm. This suggests that the practical resolution of the MR images was 0.156 mm.

While the MRI technique was capable of imaging behind the iris, around the region of contact between the iris and anterior lens surface, the two structures could not be distinguished. This required removal of these data when fitting the anterior lens surface with conic curves. Examples of conic curve fits to the anterior and posterior lens surfaces are shown in Figure 2 for one eye of a young subject in the relaxed (A) and accommodated states (B) and for one eye of an older subject (C). For the anterior lens surface, considerable data were unavailable along the region of contact between the iris and the anterior lens surface. Therefore, the conic curve fits were unreliable and the results on the anterior lens surface vertex radius of curvature and asphericity were excluded from the study. The posterior surface conic curve fits were good with r-squared values greater than 0.95 and root mean square error of less than 0.1 mm for all fits.

MRI versus A-scan measurements

MRI and applanation A-scan measurements of axial ocular dimensions were compared in all eyes of young and old subjects for the relaxed accommodative state. MRI lens thickness measurements were significantly correlated to A-scan lens thickness measurements (MRI_LT = 0.89 * AScan_LT + 0.43, r^2 = 0.90, $p < 0.01$, regression not shown). The slope of the linear regression was marginally significantly different from 1 ($p = 0.05$) and the intercept was not different from 0 ($p = 0.08$). A paired t-test revealed no significant differences between MRI and A-scan measurements (mean ± SEM: 0.05 ± 0.036 mm; $p = 0.22$). When the outlier (marked with a square in Figure 3A) was ignored in the regression analysis, the slope and intercept were not significantly different from 1 ($p = 0.14$) and 0 ($p = 0.17$), respectively, indicating good correspondence between MRI and A-scan measurements of anterior chamber depth. Bland –Altman analysis, i.e. difference between A-scan and MRI measurements plotted against the mean of A-scan and MRI measurements, showed no obvious trends in the data.

MRI axial length measurements were significantly correlated to A-scan axial length measurements (MRI_AL = 0.98 * AScan_AL + 1.37, r2 = 0.89, $p < 0.01$, Figure 3B). The slope and intercept of the linear regression were not different from 1 ($p = 0.71$) and 0 ($p = 0.39$), respectively. In the MR images, the internal boundary of the retina was not always clearly visible, so axial length measurements were performed from the anterior border of the cornea to the posterior border of the eye which would have resulted in an offset between A-scan and MRI axial length measurements. Paired differences showed

that MRI axial length measurements were larger than A-scan length measurements by 0.79 ± 0.039 mm (mean ± SEM, $p < 0.05$). The slope in Figure 3B is close to 1, indicating good correspondence between A-scan and MRI axial length measurements. Bland –Altman analysis for axial length data indicated a mean difference of 0.79 mm and no other obvious trends in the data.

Changes with Age and Accommodation

Ocular alignment during far viewing and near viewing in young subjects was checked by comparing eye rotation angle and axial lengths. No statistically significant differences were seen for eye rotation angle (paired t-test, $p = 0.99$) or axial length (paired t-test, $p = 0.13$) between unaccommodated and accommodated states. The average absolute difference in ocular alignment was 1.95 ± 1.99 degrees and absolute axial length difference was 0.13 ± 0.10 mm. While there were some differences in eye rotation angle and axial lengths between unaccommodated and accommodated images in individual eyes, these differences were not systematic.

Axial distances:

Anterior chamber depth decreased significantly with accommodation and age (Figure 4 & Table 1). On average, anterior chamber depth decreased 0.31 mm with accommodation (paired t-test, $p < 0.05$) and 0.45 mm with age (unpaired t-test, $p < 0.05$). Lens axial thickness increased 0.33 mm with accommodation ($p < 0.05$) and 0.97 mm with age ($p < 0.05$) (Table 1). The decrease in anterior chamber depth with accommodation was 92% of the increase in lens thickness, but the decrease in anterior chamber depth with age was only 46% of the increase in lens thickness. Consequently, anterior segment depth did not change significantly with accommodation ($p = 0.31$), but increased significantly with age (mean change: 0.52 mm; $p < 0.05$). The ciliary body depth did not change with accommodation ($p = 0.41$) or with age ($p = 0.71$).

Equatorial distances:

Lens equatorial diameter decreased 0.32 mm with accommodation (paired t-test, $p < 0.01$) and increased 0.28 mm with age (unpaired t-test, $p < 0.05$) (Figure 5 & Table 1). As a measure of lens shape, the ratio of lens axial thickness to equatorial

diameter (LT/ED) was calculated (Table 1). This ratio (LT/ED) increased with accommodation (mean change: 0.05; $p < 0.01$, Table 1) and age (mean change: 0.09; $p < 0.01$). An increase in LT/ED suggests that the whole lens became more rounded with accommodation and age. With accommodation, the decrease in lens equatorial diameter was 98% of the increase in lens axial thickness. With age, the increase in lens equatorial diameter was only 29% of the increase in lens axial thickness. Therefore, although the relative changes in lens thickness and equatorial diameter were different between accommodation and age, the lens assumed a more rounded shape in either case. The ciliary ring diameter decreased with both accommodation (mean change: 0.44 mm; $p < 0.05$) and age (mean change: 0.57 mm; $p < 0.05$) (Figure 5 & Table 1). The circumlental space, the distance from the equatorial edge of the lens to the ciliary body tip, did not change with accommodation (1.07 vs 1.02 mm; $p = 0.13$) but decreased significantly with age (1.07 vs 0.65 mm; mean change: 0.43 mm; $p < 0.05$).

Posterior Lens Surface Curvature and Asphericity:

The vertex radius of curvature of the posterior lens surface decreased with accommodation (mean change: 0.58 mm; $p < 0.01$) but not with age ($p = 0.21$) (Table 1). The conic constant of the posterior lens surface did not change with accommodation ($p = 0.98$) (Table 1), but increased, becoming more spherical (i.e. closer to a 'k' value of 1) with age (mean change: 0.87; $p < 0.01$).

Summary of the Results:

Table 1 provides the mean values of the various biometric parameters measured in the study. Figure 6 shows the changes in lens dimensions with accommodation (A) and age (B) using actual measured average dimensions. The data points in the figure represent mean ± 1 standard error of the mean (in most cases the error bars were smaller than the symbol size). Corneal apex for the various lens groups was fixed at '0' for reference. The curve representing the posterior crystalline lens surface was based on the average vertex curvature and average conic constant derived from equation 1. The specific changes in lens axial and equatorial dimensions, ciliary body location and posterior lens surface curvature can be seen in Figure 6.

Discussion

The MRI technique was successfully employed to study changes in crystalline lens shape with age and accommodation. The crystalline lens became thicker and more spherical in shape with both accommodation and age. However, equatorial diameter of the crystalline lens decreased with accommodation and increased with age. A significant change in the posterior surface radius of curvature was seen with accommodation. Age and accommodation related changes in crystalline lens and ciliary muscle position are discussed in detail below.

MRI accuracy and resolution

The resolution of the MRI technique was not as high as optical (< 10 microns) or ultrasound techniques (~100 microns with conventional ultrasound biometer or 2 microns with continuous high resolution biometer) (Drexler, Baumgartner, Findl, Hitzenberger, & Fercher, 1997; De Vries, Van Der Heijde, & Goovaerts, 1987). An important advantage of MRI is the unique ability to image whole lens and adnexa *in-vivo*, with ~100 micron resolution. With blinks and eye movements, it was possible in this study to detect changes of about 156 microns (see Results – Resolution and noise level). One of the aims of the study was to describe the three dimensional shape of the lens by obtaining images along sagittal and transverse axial sections. Unfortunately, the sagittal images were noisier than the transverse axial images, possibly due to eye movements and blinks. In the interest of accuracy, only results from the transverse axial images have been provided. At the region of contact between the iris and the anterior crystalline lens surface, the two surfaces were indistinguishable leading to exclusion of the anterior lens surface data from further analysis (Figure 2). The radius of curvature and asphericity values for the posterior lens surface alone are provided.

Axial Distances

As reported previously, anterior chamber depth decreased with accommodation and age and the lens thickness increased with accommodation and age (see Table 1 & Figure 4) (Bolz, Prinz, Drexler, & Findl, 2007; Drexler, et al., 1997; Dubbelman, Van der Heijde, & Weeber, 2005; Garner & Yap, 1997; Koeppl, Findl, Kriechbaum, & Drexler, 2005; Koretz,

Cook, & Kaufman, 1997; Ostrin, Kasthurirangan, Win-Hall, & Glasser, 2006; Tsorbatzoglou, Nemeth, Szell, Biro, & Berta, 2007; Atchison, et al., 2008; Cook, Koretz, Pfahnl, Hyun, & Kaufman, 1994; Dubbelman, et al., 2001; Kashima, Trus, Unser, Edwards, & Datiles, 1993; Koretz, et al., 1989; Koretz, Strenk, Strenk, & Semmlow, 2004; Hermans, Pouwels, Dubbelman, Kuijer, van der Heijde, & Heethaar, 2009; Jones, et al., 2007; Kasthurirangan, Markwell, Atchison, & Pope, 2008; Richdale, Bullimore, & Zadnik, 2008; Strenk, et al., 1999). The anterior segment depth did not change with accommodation, but increased with age (Figure 4). With accommodation, the decrease in anterior chamber depth (0.31 mm) was similar to the increase in lens thickness (0.33 mm), leading to no change in anterior segment depth. A drawback of the current study was the inability to measure accommodative response in diopters during MR imaging. However, an increase in lens thickness of 0.33 mm would correspond to an accommodative response of 4.92 D using the lens thickness change to accommodation ratio of 0.067 mm/D reported by Ostrin et al (2006).. The mean accommodative changes reported in the current study correspond to about 5 D of response accommodation. With aging, the increase in lens thickness (0.97 mm or 0.02 mm/year) was twice the decrease in anterior chamber depth (0.45 mm or 0.01 mm/year) and twice the increase in anterior segment length (0.52 mm or 0.01 mm/year) (Atchison, et al., 2008).

Some previous studies have reported that anterior segment depth increases with accommodation (Bolz, et al., 2007; Drexler, et al., 1997; Dubbelman, et al., 2005; Ostrin, et al., 2006). Koeppl et al (2005) did not find this with partial coherence interferometry although two other studies using the same technique did find an increase (Bolz, et al., 2007; Drexler, et al., 1997). The increase in anterior segment depth reported in these studies, for ~5 D accommodation, ranged from 0.04 to 0.09 mm. A possible reason for the lack of significant change in anterior segment depth in the present study could be due to the resolution limits of the MRI technique (0.156 mm) as the expected changes are only 0.1 mm or less. Another plausible reason, given the similar magnitude of change in anterior chamber depth and lens thickness, could be the supine posture of the subjects compared to the erect posture of subjects in past studies (personal communication with Dr. Adrian Glasser). In a supine posture, the crystalline lens may sag to its deepest position due to the effect of gravity, even in the unaccommodated state. Therefore, with accommodation, no further backward movement could have been possible. In the present study anterior chamber and segment depths measured in erect posture using an A-scan ultrasound were significantly smaller than the supine MRI measured values, with mean differences (paired t-tests; $p < 0.05$) of 0.12 and 0.11

mm respectively. However, lens thickness was not different between erect and supine measurements (paired t-test; $p = 0.22$). The difference between MRI and A-scan measured anterior segment depths is similar to the expected accommodative change (up to 0.10 mm). This lends support to the idea that erect vs supine posture of the subjects may determine whether or not anterior segment depth changes during accommodation. It is of interest to evaluate this effect of lens position during erect and supine postures and with accommodation in a future study.

A significant change in posterior lens surface radius of curvature was seen with accommodation. Therefore, although there is no posterior movement of the posterior pole of the lens in this study (i.e. no change in anterior segment depth), the posterior surface of the lens actively participated in the accommodative process.

Equatorial Lens Diameter and Shape

Similar to previous reports, the equatorial diameter of the lens decreased with accommodation (Glasser, Wendt, & Ostrin, 2006; Strenk, et al., 1999; Wendt, Croft, McDonald, Kaufman, & Glasser, 2008) (Table 1 & Figure 5). In the current study, the decrease in equatorial diameter (0.32 mm) was equivalent to the increase in axial thickness of the lens (0.33 mm). Also, the ratio of crystalline lens thickness to diameter increased, approaching 0.5, indicating that the crystalline lens became more rounded with accommodation. It is interesting to note the similarity in magnitude of the change in lens axial thickness and equatorial diameter for a certain magnitude of accommodative response, suggesting that the changes in the two parameters per diopter of accommodation may also be equivalent.

A significant increase in crystalline lens diameter with age was seen. The change in equatorial diameter (0.28 mm, 0.007 mm/year) was only 1/3rd of the increase in crystalline lens thickness (0.97 mm) with age. Previous reports have shown no change in crystalline lens equatorial diameter with age in humans (Strenk, et al., 1999) or Rhesus monkeys (Wendt, et al., 2008). In the present study mean crystalline lens diameters in two groups of subjects separated in age by about 40 years were compared. In past reports linear regression analysis was undertaken to study age-related changes in lens diameter (Strenk, et al., 1999; Wendt, et al., 2008). The magnitude of the changes reported in the present study could have been missed in past studies using regression analysis, due to the wide individual variation and lack of sufficient subjects in clearly delineated age

groups. A potential confounding factor leading to the observed age-related changes in equatorial diameter in the current study could have been the level of tonic accommodation in the younger subjects even when a far target was used to relax accommodation. This and previous studies measured unaccommodated lens diameters during far viewing and without any cycloplegic agent (Strenk, et al., 1999; Wendt, et al., 2008). A greater baseline tonic accommodation in younger subjects (leading to decrease in lens diameter) compared to older subjects could have resulted in an increase in lens diameter with age as seen in the current study. Nevertheless, present study is comparable to past studies because none of the studies used a cycloplegic agent. A future study should consider using cycloplegic agents to truly measure changes in unaccommodated lens equatorial diameter with age.

The increase in the lens thickness to equatorial diameter ratio shows that the crystalline lens becomes more rounded with age. Across vertebrate species a flattened lens shape in the unaccommodated state leads to greater change in lens shape with an effort to accommodate (Fisher, 1969; Schachar, Pierscionek, Abolmaali, & Le, 2007). Schachar suggested that lens central thickness to lens equatorial diameter ratio of ≤0.60 is commonly seen in animals that have the capacity to accommodate (Schachar, et al., 2007). In the current study, while the LT/ED ratio of the crystalline lens increases with age (0.50 at 65 years of age compared to 0.41 at 22 years), it is still within the limits seen for accommodating animal species (i.e. ≤0.60). Interestingly, the LT/ED ratio of the older lenses (0.50) is similar to the fully accommodated young crystalline lens (0.46), suggesting that there may be some decrease in accommodative functionality due to lens growth. The relatively spherical shape of the unaccommodated crystalline lens in older subjects and any associated changes with age in the geometric relationship between ciliary muscle and lens (Koretz & Handelman, 1988; Strenk, Strenk, & Koretz, 2005) may contribute to a faster decline in accommodative amplitude with the progression of presbyopia, even though the ultimate cause may still be increased lens stiffness (Atchison, 1995; Fisher, 1973; Glasser & Campbell, 1999; Heys, Cram, & Truscott, 2004; van Alphen & Graebel, 1991; Weeber, Eckert, Soergel, Meyer, Pechhold, & van der Heijde, 2005).

Ciliary Body Movement

Only a few studies have reported ciliary body/ciliary muscle movement with accommodation and age, especially in humans. In the current study no forward movement of the ciliary body was observed with accommodation or aging (Table

1). The lack of forward movement of the ciliary body with accommodation is in accordance with two studies in humans (Baikoff, Lutun, Wei, & Ferraz, 2004; Strenk, Strenk, & Guo, 2010),) while ultrasound imaging in humans and Rhesus monkeys have shown forward movement of the ciliary muscle apex with accommodation (Stachs, et al., 2002; Croft, Glasser, Heatley, McDonald, Ebbert, Dahl, Nadkarni & Kaufman, 2006). An MRI study in humans showed a more forward positioning of the ciliary muscle with age (0.009 mm per year; Strenk, et al., 2010), which was not seen in the current study. It is likely that the lack of any measurable forward ciliary movement during accommodation or with age in the current study was due to the limited resolution of our MRI technique (0.156 mm).

Centripetal movement (i.e. decrease in ciliary ring diameter) was observed with accommodation and aging similar to previous studies (Baikoff, et al., 2004; Strenk, et al., 1999; Strenk, Strenk, & Guo, 2006) (Table 1 & Figure 5). The circumlental space, the space between lens equatorial edge and ciliary body tip, did not change with accommodation and decreased with age as shown previously in humans (Strenk, et al., 2006) and Rhesus monkeys (Glasser, Croft, Brumback, & Kaufman, 2001). In young Rhesus monkeys the circumlental space has been shown to remain stable or decrease only slightly during Edinger Westphal (EW) nucleus stimulated accommodation, while significant changes were observed during supra-maximal or pharmacological (eg: carbachol) stimulation of accommodation (Ostrin & Glasser, 2007). The lack of changes in circumlental space in young humans in the current study may be because the ciliary muscle effort was within the maximum accommodative amplitude of the subjects.

Circumlental space decreased by 40% over the 40 year age gap between young and older subjects. This decrease was due to a combination of increase in lens equatorial diameter (0.28 mm) and decrease in ciliary ring diameter (0.57 mm) leading to 0.43 mm decrease in circumlental space. Following cataract surgery, the ciliary body has been shown to move outward (i.e. towards its position in young humans) (Strenk, et al., 2010). This observation, along with the findings of the current study, suggests that the axial growth of the lens with age may increase the natural tension in the anterior zonular fibers during relaxed accommodation, in turn exerting an inward pull on the ciliary body leading to a reduction in circumlental space. This force may be partly or fully released following cataract surgery due to the removal of lens material and collapse of the capsular bag. The magnitude of the re-positioning of the ciliary muscle following cataract surgery will be quite informative in determining the success of accommodating IOLs.

Lens Surface Curvature and Asphericity

The objective of the current study was to describe the overall biometric shape of the lens surface and not a central optically relevant region. All previous studies on the lens surface shape had considered only a central zone and are not directly comparable to the current study. With accommodation, the radius of curvature of the posterior lens surface decreased as reported previously with a variety of optical methods in humans and Rhesus monkeys (Brown, 1973; Dubbelman, et al., 2005; Garner & Yap, 1997; Kirschkamp, Dunne, & Barry, 2004; Koretz, et al., 1987; Koretz, Cook, & Kaufman, 2002; Rosales, Dubbelman, Marcos, & van der Heijde, 2006; Rosales, Wendt, Marcos, & Glasser, 2008) (Table 1). The conic constant of the posterior surface did not change with accommodation (Table 1). Previous studies were based on optical techniques and it was not clear if the observed changes in the posterior lens surface were due to any optical artefacts when measuring through an accommodating lens. The current study has used MRI to demonstrate clear changes in the posterior lens surface during accommodation using a non-optical imaging technique. The anterior lens surface curvature could not be reliably measured in the current study primarily due to the loss of data at the region of contact between the iris and anterior lens surface.

With age, the radius of curvature of the posterior lens surface did not change and the conic constant increased. The trends in radius of curvature are largely supported by literature (Atchison, et al., 2008; Brown, 1973; Koretz, et al., 2004), with only two studies showing some decrease in posterior lens radius with age (Dubbelman & Van Der Heijde, 2001; Koretz, Cook, & Kaufman, 2001). The mean posterior lens radius of curvature of 6.08 mm is at the lower end of past reports of 5.6 mm to 7.7 mm (Koretz, et al., 2004, Koretz, et al., 2004, Dubbelman & Van Der Heijde, 2001, Atchison, et al., 2008, Brown, 1973). Dubbelman et al (2001) reported no changes in the conic constant of the posterior surface with age. It is difficult to compare the findings of the current study directly with Dubbelman et al's Scheimpflug measurements because of the differences in lens zone diameter considered and the potential influence of the optical technique on posterior lens surface measurements. The current study shows that the posterior lens surface becomes more spherical with age.

Mechanism of Accommodation

The various changes in the crystalline lens identified during accommodation are shown in Figure 6A based on the mean data from Table 1. During accommodation, the anterior chamber depth decreases, the crystalline lens increases in thickness and decreases in diameter with a reduction in the radius of curvature of the posterior lens surface. The increase in lens thickness is equal to the decrease in anterior chamber depth with no change in anterior segment depth. The decrease in equatorial diameter is equal in magnitude to the increase in lens thickness. The ciliary body moves inward without any forward movement, while the circumlental space remains unchanged. The lenticular findings strongly support the Helmholtz theory of accommodation with clear demonstration of the role of the posterior surface during accommodation. The lack of any decrease in circumlental space for maximum accommodation, combined with past reports of a decrease in circumlental space with supramaximal stimulation (Ostrin & Glasser, 2007), suggest that maximum accommodation in conscious young humans is achieved with ciliary muscle effort in reserve, supporting the Hess-Gullstrand theory which is that the amount of ciliary muscle contraction required for a given change in accommodation response remains the same throughout life (Atchison, 1995; Eskridge, 1984; Gullstrand, 1924).

Mechanism of Presbyopia

The various changes in the crystalline lens with age are shown in Figure 6B using mean data from Table 1. Age-related crystalline lens growth leads to a decrease in anterior chamber depth, an increase in lens thickness three (3) times more than the increase in lens diameter and no change in the vertex radius of curvature of the posterior lens surface. The increase in lens thickness manifests as a similar decrease in anterior chamber depth and an increase in anterior segment depth. Since lens thickness increases significantly more than the lens diameter, the ratio of thickness to diameter increases with age (approaching 0.50). The posterior lens asphericity approached '1' i.e. towards spherical surfaces. The ciliary body moves inward with no forward movement.

A majority of the age-related lenticular changes and the ciliary body position mimic accommodative changes suggesting that the decline in accommodative amplitude with presbyopia may be accelerated by age-related changes in lens shape and ciliary body position (i.e. inward movement). A recent study reported that the ciliary body undergoes a centrifugal

movement following cataract surgery (Strenk, et al., 2010),) presumably due to the release in inward forces on the ciliary body after removal of a cataractous and presbyopic crystalline lens. Such a change, if consistently demonstrated, will increase the promise of presbyopia reversal procedures in restoring useful accommodation. An important outcome of this study is the age-related normative values given in Table 1, that will help in planning accommodating-IOL designs and presbyopia reversal procedures to better suit the accommodative anatomy of older patients undergoing cataract surgery to maximize accommodative potential.

Figures

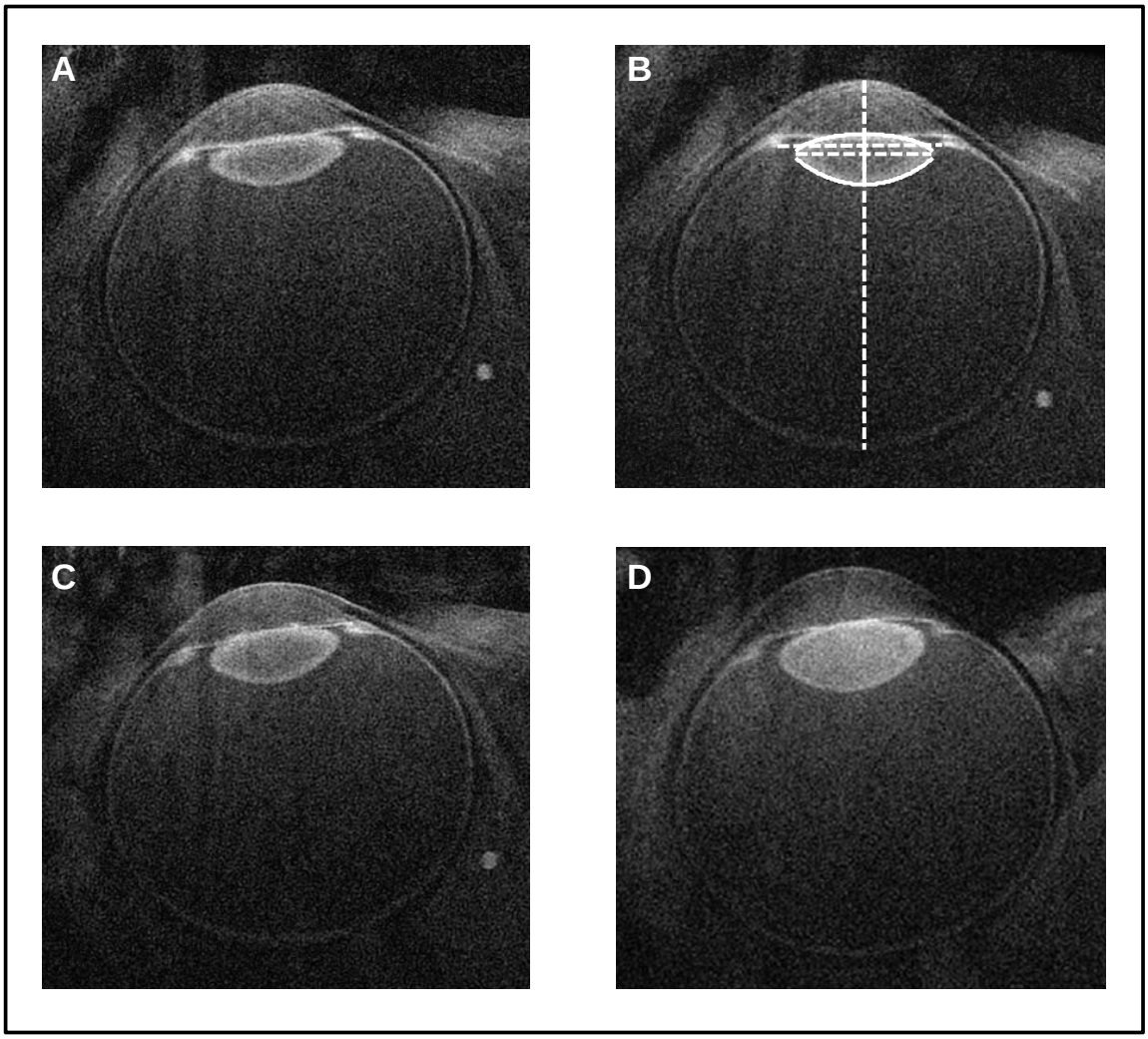

Figure 1. (A) Transverse axial MR image of a 23 year old subject during far viewing. (B) The same image has been rotated using custom developed Matlab software to orient the eye with cornea above, sclera below and a horizontal crystalline lens with no tilt. Dashed white lines indicate various automatically measured intra-ocular dimensions including anterior chamber depth, lens thickness, lens diameter, ciliary ring diameter and axial length. Conic curve fits to lens surfaces are indicated by thick white lines. (C) MR image of the same 23 year old subject during near viewing. (D) MR image of a 65 year old subject during far viewing.

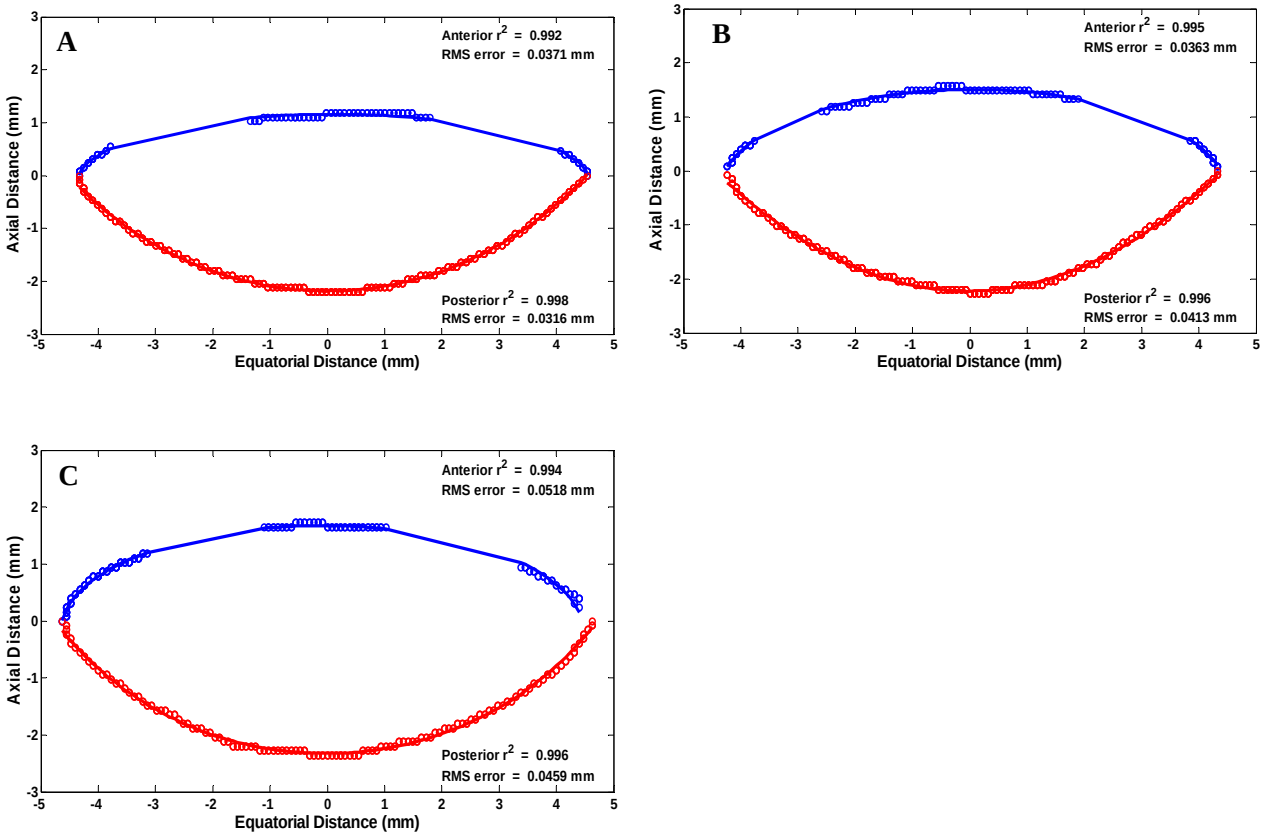

Figure 2: Examples of conic curve fits to anterior and posterior lens surfaces in one eye of a young subject during relaxed (A) and accommodated (B) states, and in one eye of an older subject during relaxed state (C). These examples represent posterior lens radius of curvature values close to the average value within each condition. The anterior lens surface fits suffered from missing data at the region of contact between the iris and the crystalline lens. Results on anterior lens surface fits were excluded from the study. The posterior lens surface fits were excellent with r-squared values greater than 0.95 and rms fit error less than 0.1 mm.

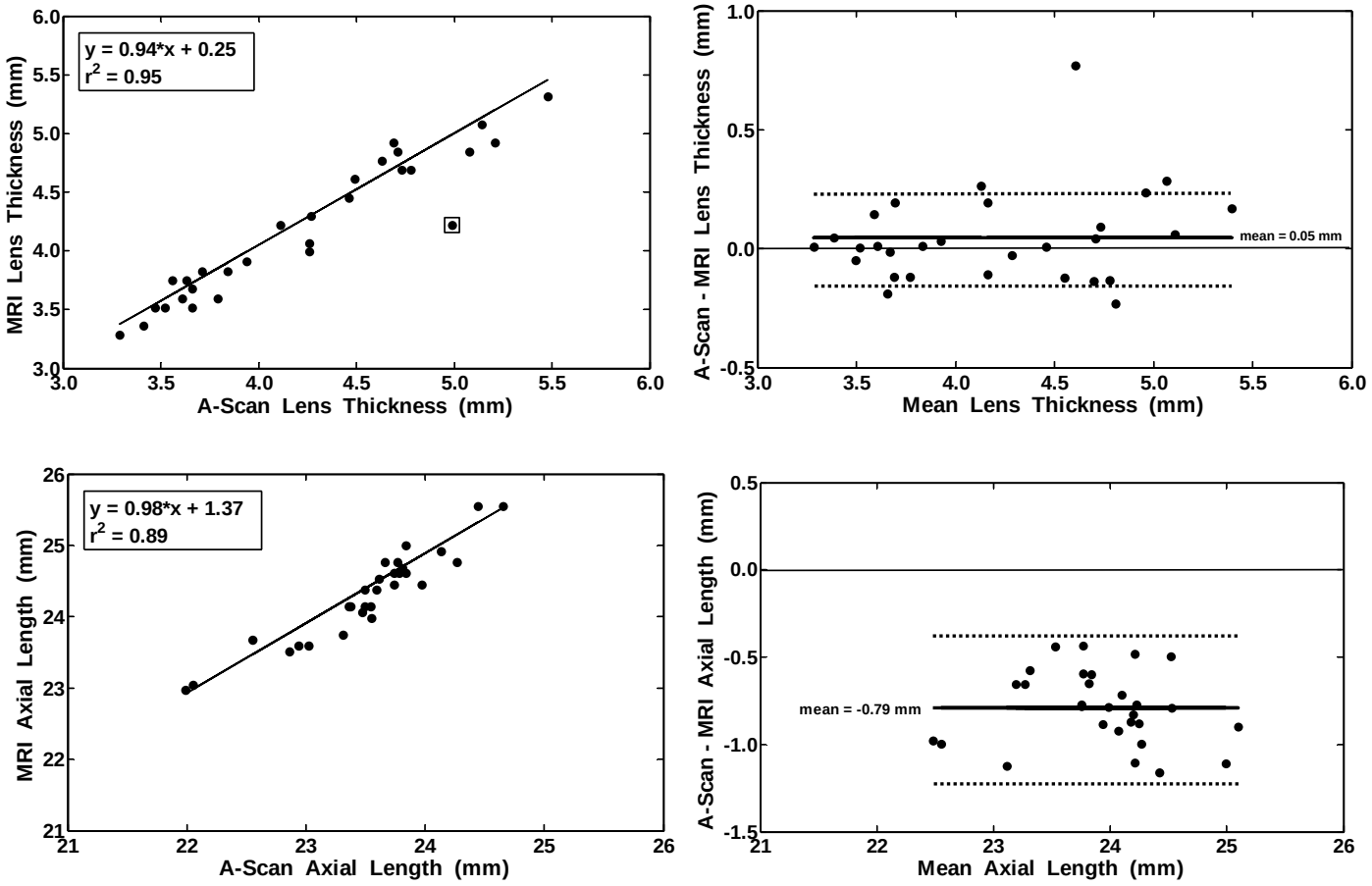

Figure 3. (A) Lens thickness measured with A-scan (X-axis) and MRI (Y-axis) show good correlation, albeit with one outlier marked in a square. A significant linear relationship (excluding the outlier) was found with slope not different from 1 and intercept not different from zero. No difference was seen between the two data sets based on a paired t-test (p = 0.22). (B) Bland-Altman analysis of lens thickness data showed a mean difference close to zero and no obvious trends. (C) Axial length measured with A-scan (X-axis) and MRI (Y-axis) show good correlation with slope not different from one and intercept not different from zero. (D) Bland –Altman analysis of axial length data showed that, on average, MRI measurements were 0.79 mm larger than A-scan values, with no other obvious trends in the data.

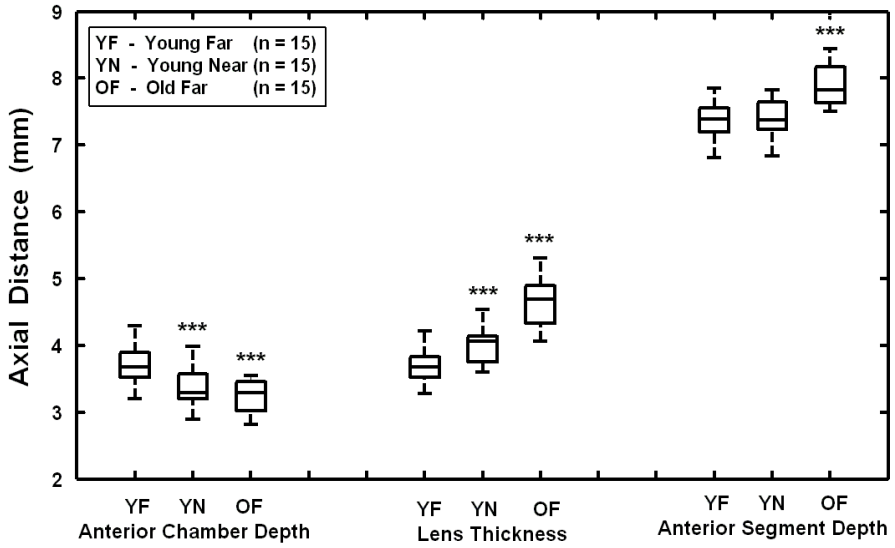

Figure 4. Box plot showing median and range of axial distances of anterior chamber depth, lens thickness and anterior segment length for young subjects during far viewing (YF) and near viewing (YN),) and for older subjects during far viewing (OF). Statistically significant differences in means from YF data are indicated with '***'. Anterior chamber depth decreased with accommodation and age. Lens thickness increased with accommodation and age. Anterior segment length did not change with accommodation, but increased with age.

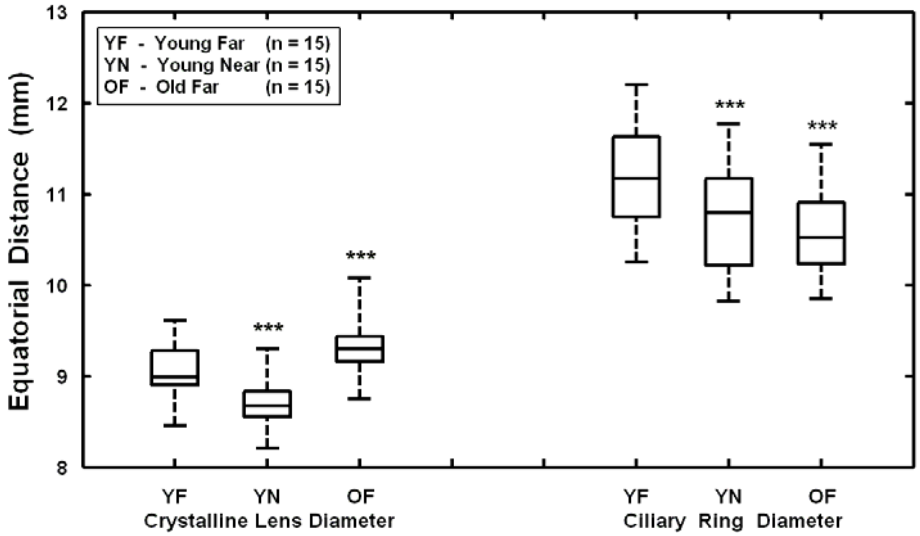

Figure 5. Box plot showing median and range of equatorial values of crystalline lens diameter and ciliary ring diameter for young subjects during far viewing (YF) and near viewing (YN),) and for older subjects during far viewing (OF). Statistically significant differences in means from YF data are indicated with '***'. Lens diameter decreased with accommodation and increased with age. Ciliary ring diameter decreased with accommodation and age.

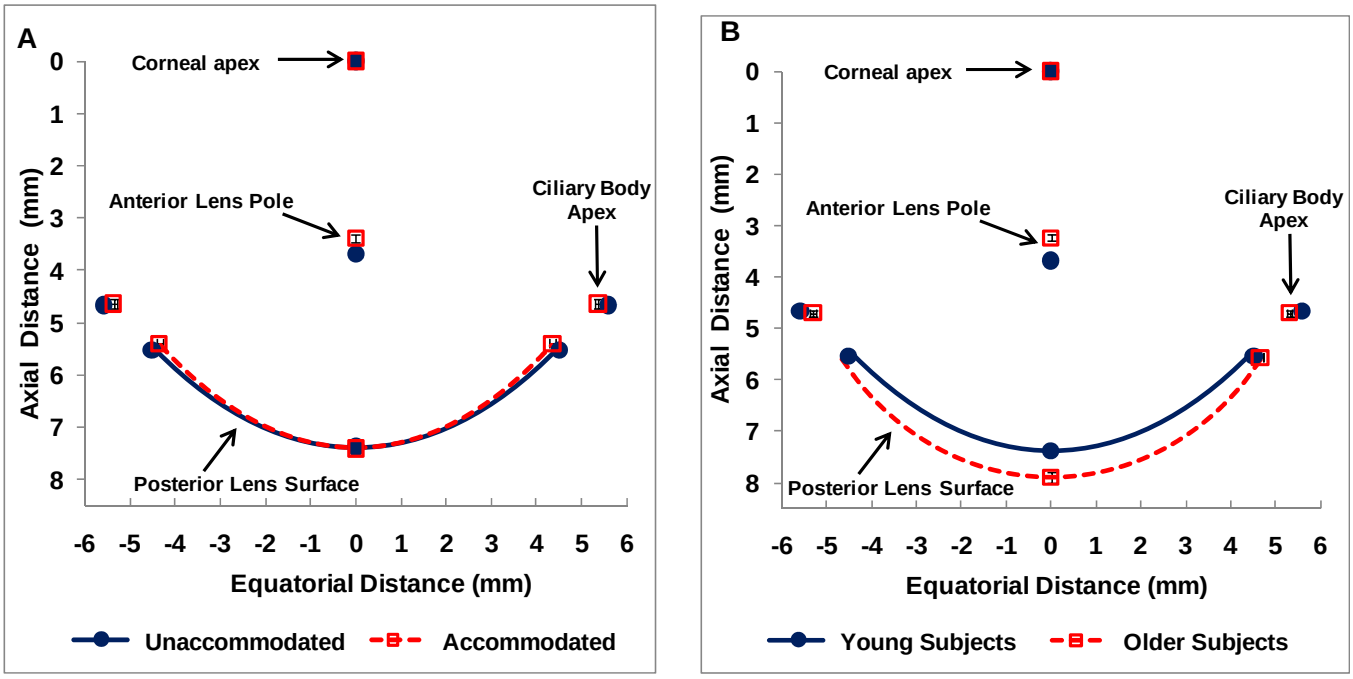

Figure 6. Changes in crystalline lens and ciliary body apex with accommodation (A) and age (B). In (A),, the corneal apex is fixed at '0' for unaccommodated (filled circle and solid lines in blue) and accommodated (open square and dashed lines in red) conditions. The data points are mean ± 1 SEM values and the lines indicating lens surfaces are based on mean radii of curvature and conic constants. In (B),data for older subjects (open square and dashed lines in red) are plotted using the same scheme as (A).. The overall changes in lens size and shape can be observed in the figures. The anterior lens surface could not be well fit with conic curves due to missing data at the region of iris overlap. The anterior pole of the crystalline lens moved forward with accommodation and aging. The ciliary body apex moved inward with accommodation and age, but no forward movement in either case was observed.

Tables

Parameter	Young Far	Young Near	Older Far
	mean (SD)	mean (SD)	mean (SD)
Age (years)	22.32 (3.39)	22.32 (3.39)	63.61* (3.09)
Axial Length (mm)	24.27 (0.79)	24.20 (0.76)	24.36 (0.41)
Anterior Chamber Depth (mm)	3.69 (0.29)	3.38* (0.30)	3.24* (0.25)
Lens Thickness (mm)	3.69 (0.25)	4.02* (0.27)	4.66* (0.36)
Anterior Segment Depth (mm)	7.38 (0.28)	7.40 (0.28)	7.90* (0.31)
Ciliary Body Depth (mm)	4.66 (0.29)	4.64 (0.30)	4.70 (0.24)
Lens Equatorial Diameter (mm)	9.03 (0.30)	8.71* (0.29)	9.31* (0.29)
Lens Thickness/ Equatorial Diameter	0.41 (0.03)	0.46* (0.04)	0.50* (0.05)
Ciliary Ring Diameter (mm)	11.18 (0.54)	10.74* (0.59)	10.61* (0.49)
Posterior Surface Radius of Curvature (mm)	-5.66 (1.00)	-5.08* (0.71)	-6.08 (0.74)
Posterior Surface Conic Constant 'K'	0.22 (0.64)	0.22 (0.57)	1.09* (0.44)

Table 1. Mean (± SD) values for biometric parameters measured from transverse axial MR images for young subjects during far and near viewing and older subjects during far viewing. Statistically significant differences from young far viewing data for each parameter are indicated with '*'.

Acknowledgment

This work was supported by National Health and Medical Research Council Grant 290500. We thank the reviewers for their insightful suggestions to improve the quality of the manuscript.

Commercial relationships: None.

Corresponding author: Sanjeev Kasthurirangan

Email: sanjeev.k@amo.abbott.com

Address: 510 Cottonwood Dr., Milpitas, CA 95035, USA

References

Atchison, D. A. (1995). Accommodation and presbyopia. *Ophthalmic and Physiological Optics, 15*(4), 255-272.

Atchison, D. A., Markwell, E. L., Kasthurirangan, S., Pope, J. M., Smith, G., & Swann, P. G. (2008). Age-related changes in optical and biometric characteristics of emmetropic eyes. *Journal of Vision, 8*(4), 29, 1-20.

Atchison, D. A., & Smith, G. (2004). Possible errors in determining axial length changes during accommodation with the IOLMaster. *Optometry and Vision Science, 81*(4), 282-285.

Baikoff, G., Lutun, E., Wei, J., & Ferraz, C. (2004). Anterior chamber optical coherence tomography study of human natural accommodation in a 19-year-old albino. *Journal of Cataract and Refractive Surgery, 30*(3), 696-701.

Beers, A. P., & Van Der Heijde, G. L. (1994). Presbyopia and velocity of sound in the lens. *Optometry and Vision Science, 71*(4), 250-253.

Beers, A. P. A., & Van Der Heijde, G. L. (1994). In vivo determination of the biomechanical properties of the component elements of the accommodative mechanism. *Vision Research, 34*(21), 2897-2905.

Bland, J. M., & Altman, D. G. (1986). Statistical methods for assessing agreement between two methods of clinical measurement. *Lancet,* 1(8476):307-10.

Bolz, M., Prinz, A., Drexler, W., & Findl, O. (2007). Linear relationship of refractive and biometric lenticular changes during accommodation in emmetropic and myopic eyes. *British Journal of Ophthalmology, 91*(3), 360-365.

Brown, N. (1973). The change in shape and internal form of the lens of the eye on accommodation. *Experimental Eye Research, 15,* 441-459.

Cook, C. A., Koretz, J. F., Pfahnl, A., Hyun, J., & Kaufman, P. L. (1994). Aging of the human crystalline lens and anterior segment. *Vision Research, 34(22),* 2945-2954.

Croft, M.A., Glasser, A., Heatley, G., McDonald, J., Ebbert, T., Dahl, D. B., Nadkarni, N. V., Kaufman, P. L. (2006). Accommodative ciliary body and lens function in Rhesus monkeys, I: Normal lens, zonule and ciliary process configuration in the iridectomized eyes. *Investigative Ophthalmology and Visual Science, 47*(3), 1076-1086.

Cumming, J. S., Slade, S. G., & Chayet, A. (2001). Clinical evaluation of the model AT-45 silicone accommodating intraocular lens: results of feasibility and the initial phase of a Food and Drug Administration clinical trial. *Ophthalmology, 108*(11), 2005-2009.

De Vries, F. R., Van Der Heijde, G. L., & Goovaerts, H. G. (1987). System for continuous high-resolution measurement of distances in the eye. *Journal of Biomedical Engineering, 9*(January), 32-37.

Demer, J. L., Clark, R. A., Crane, B. T., Tian, J. R., Narasimhan, A., & Karim, S. (2008). Functional anatomy of the extraocular muscles during vergence. *Progress in Brain Research, 171*, 21-28.

Dick, H. B. (2005). Accommodative intraocular lenses: current status. *Current Opinion in Ophthalmology, 16*(1), 8-26.

Drexler, W., Baumgartner, A., Findl, O., Hitzenberger, C. K., & Fercher, A. F. (1997). Biometric investigation of changes in the anterior eye segment during accommodation. *Vision Research, 37*(19), 2789-2800.

Duane, A. (1912). Normal values of the accommodation at all ages. *Journal of the American Medical Association*(Sept.), *59(12),* 1010-1013.

Dubbelman, M., & Van Der Heijde, G. L. (2001). The shape of the aging human lens: curvature, equivalent refractive index and the lens paradox. *Vision Research, 41*(14), 1867-1877.

Dubbelman, M., Van Der Heijde, G. L., & Weeber, H. A. (2001). The thickness of the aging human lens obtained from corrected Scheimpflug images. *Optometry and Vision Science, 78*(6), 411-416.

Dubbelman, M., Van der Heijde, G. L., & Weeber, H. A. (2005). Change in shape of the aging human crystalline lens with accommodation. *Vision Research, 45*(1), 117-132.

Eskridge, J. B. (1984). Review of ciliary muscle effort in presbyopia. *American Journal of Optometry, 61*(2), 133-138.

Fisher, R. F. (1969). The significance of the shape of the lens and capsular energy changes in accommodation. *The Journal of Physiology, 201,* 21-47.

Fisher, R. F. (1973). Presbyopia and the changes with age in the human crystalline lens. *The Journal of Physiology, 228,* 765-779.

Garner, L. F., & Yap, M. K. H. (1997). Changes in ocular dimensions and refraction with accommodation. *Ophthalmic and Physiological Optics, 17*(1), 12-17.

Glasser, A., & Campbell, M. C. W. (1999). Biometric, optical and physical changes in the isolated human crystalline lens with age in relation to presbyopia *Vision Research, 39*(11), 1991-2015.

Glasser, A., Croft, M. A., Brumback, L., & Kaufman, P. L. (2001). Ultrasound biomicroscopy of the aging rhesus monkey ciliary region *Optometry and Vision Science, 78*(6), 417-424.

Glasser, A., & Kaufman, P. L. (1999). The mechanism of accommodation in primates *Ophthalmology, 106*(5), 863-872.

Glasser, A., Wendt, M., & Ostrin, L. (2006). Accommodative changes in lens diameter in rhesus monkeys. *Investigative Ophthalmology and Visual Science, 47*(1), 278-286.

Gullstrand, A. (1924). The mechanism of accommodation. Appendix IV in *Helmholtz's Treatise on Physiological Optics* Vol. 1, 3rd edition. English Translation edited by J. P. C. Southall (Ed.), New York: Optical Society of America, (pp. 382-415).

Helmholtz von, H.H. (1924). Mechanism of accommodation. In: Southall JPC (ed), *Helmholtz's Treatise on Physiological Optics*. New York: Optical Society of America;1924:143-173.

Hermans, E. A., Pouwels, P. J., Dubbelman, M., Kuijer, J. P., van der Heijde, R. G., & Heethaar, R. M. (2009). Constant volume of the human lens and decrease in surface area of the capsular bag during accommodation: an MRI and Scheimpflug study. *Investigative Ophthalmology and Visual Science, 50*(1), 281-289.

Heys, K. R., Cram, S. L., & Truscott, R. J. (2004). Massive increase in the stiffness of the human lens nucleus with age: the basis for presbyopia? *Molecular Vision, 10,* 956-963.

Ho, A., Manns, F., Pham, T., & Parel, J. M. (2006). Predicting the performance of accommodating intraocular lenses using ray tracing. *Journal of Cataract and Refractive Surgery, 32*(1), 129-136.

Jones, C. E., Atchison, D. A., & Pope, J. M. (2007). Changes in lens dimensions and refractive index with age and accommodation. *Optometry and Viions Science, 84*(10), 990-995.

Kashima, K., Trus, B. L., Unser, M., Edwards, P. A., & Datiles, M. B. (1993). Aging studies on normal lens using the Scheimpflug slit-lamp camera. *Investigative Ophthalmology and Visual Science, 34*(1), 263-269.

Kasthurirangan, S., Markwell, E. L., Atchison, D. A., & Pope, J. M. (2008). In vivo study of changes in refractive index distribution in the human crystalline lens with age and accommodation. *Investigative Ophthalmology and Visual Science, 49*(6), 2531-2540.

Kirschkamp, T., Dunne, M., & Barry, J. C. (2004). Phakometric measurement of ocular surface radii of curvature, axial separations and alignment in relaxed and accommodated human eyes. *Ophthalmic and Physiological Optics, 24*(2), 65-73.

Koeppl, C., Findl, O., Kriechbaum, K., & Drexler, W. (2005). Comparison of pilocarpine-induced and stimulus-driven accommodation in phakic eyes. *Experimental Eye Research, 80*(6), 795-800.

Koopmans, S. A., Terwee, T., Barkhof, J., Haitjema, H. J., & Kooijman, A. C. (2003). Polymer refilling of presbyopic human lenses in vitro restores the ability to undergo accommodative changes *Investigative Ophthalmology and Visual Science, 44* (1), 250-257.

Koopmans, S. A., Terwee, T., Glasser, A., Wendt, M., Vilupuru, A. S., van Kooten, T. G., et al. (2006). Accommodative lens refilling in rhesus monkeys. *Investigative Ophthalmology and Visual Science, 47*(7), 2976-2984.

Koretz, J. F., Bertasso, A. M., Neider, M. W., True-Gabelt, B., & Kaufman, P. L. (1987). Slit-lamp studies of the rhesus monkey eye. II Changes in crystalline lens shape, thickness and position during accommodation and aging. *Experimental Eye Research, 45*, 317-326.

Koretz, J. F., Cook, C. A., & Kaufman, P. L. (1997). Accommodation and presbyopia in the human eye. Changes in the anterior segment and crystalline lens with focus. *Investigative Ophthalmology and Visual Science, 38*(3), 569-578.

Koretz, J. F., Cook, C. A., & Kaufman, P. L. (2001). Aging of the human lens: changes in lens shape at zero-diopter accommodation. *Journal of the Optical Society of America A, Optics, Image Science, and Vision, 18*(2), 265-272.

Koretz, J. F., Cook, C. A., & Kaufman, P. L. (2002). Aging of the human lens: changes in lens shape upon accommodation and with accommodative loss. *Journal of the Optical Society of America A, Optics, Image Science, and Vision, 19*(1), 144-151.

Koretz, J. F., & Handelman, G. H. (1988). How the human eye focuses. *Scientific American, 259*, 92-99.

Koretz, J. F., Kaufman, P. L., Neider, M. W., & Goeckner, P. A. (1989). Accommodation and presbyopia in the human eye - aging of the anterior segment. *Vision Research, 29*(12), 1685-1692.

Koretz, J. F., Strenk, S. A., Strenk, L. M., & Semmlow, J. L. (2004). Scheimpflug and high-resolution magnetic resonance imaging of the anterior segment: a comparative study. *Journal of the Optical Society of America A, Optics, Image Science, and Vision, 21*(3), 346-354.

Krueger, R. R., Sun, X. K., Stroh, J., & Myers, R. (2001). Experimental increase in accommodative potential after neodymium: yttrium-aluminum-garnet laser photodisruption of paired cadaver lenses. *Ophthalmology, 108*(11), 2122-2129.

Mastropasqua, L., Toto, L., Nubile, M., Falconio, G., & Ballone, E. (2003). Clinical study of the 1CU accommodating intraocular lens. *Journal of Cataract and Refractive Surgery, 29* (7), 1307-1312.

Nishi, O., Hara, T., Sakka, Y., Hayashi, F., Nakamae, K., & Yamada, Y. (1992). Refilling the lens with a inflatable endocapsular balloon: surgical procedure in animal eyes. *Graefes Archives of Clinical and Experimental Ophthalmology, 230*(1), 47-55.

Ostrin, L., Kasthurirangan, S., Win-Hall, D., & Glasser, A. (2006). Simultaneous measurements of refraction and A-scan biometry during accommodation in humans. *Optometry and Vision Science, 83*(9), 657-665.

Ostrin, L. A., & Glasser, A. (2007). Edinger-Westphal and pharmacologically stimulated accommodative refractive changes and lens and ciliary process movements in rhesus monkeys. *Experimental Eye Research, 84*(2), 302-313.

Parel, J. M., Gelender, H., Trefers, W. F., & Norton, E. W. (1986). Phaco-Ersatz: cataract surgery designed to preserve accommodation. *Graefes Archives of Clinical and Experimental Ophthalmology, 224*(2), 165-173.

Richdale, K., Bullimore, M. A., & Zadnik, K. (2008). Lens thickness with age and accommodation by optical coherence tomography. *Ophthalmic and Physiological Optics, 28*(5), 441-447.

Rosales, P., Dubbelman, M., Marcos, S., & van der Heijde, R. (2006). Crystalline lens radii of curvature from Purkinje and Scheimpflug imaging. *Journal of Vision, 6*(10), 1057-1067.

Rosales, P., & Marcos, S. (2006). Phakometry and lens tilt and decentration using a custom-developed Purkinje imaging apparatus: validation and measurements. *Journal of the Optical Society of America A, Optics, Image Science, and Vision, 23*(3), 509-520.

Rosales, P., Wendt, M., Marcos, S., & Glasser, A. (2008). Changes in crystalline lens radii of curvature and lens tilt and decentration during dynamic accommodation in rhesus monkeys. *Journal of Vision, 8*(1), 18, 1-12.

Schachar, R. A., Pierscionek, B. K., Abolmaali, A., & Le, T. (2007). The relationship between accommodative amplitude and the ratio of central lens thickness to its equatorial diameter in vertebrate eyes. *British Journal of Ophthalmology, 91*(6), 812-817.

Smith, G., & Garner, L. F. (1996). Determination of the radius of curvature of the anterior lens surface from the Purkinje images. *Ophthalmic and Physiological Optics, 16*(2), 135-143.

Stachs, O., Martin, H., Kirchhoff, A., Joachim, S., Terwee, T., & Guthoff, R. (2002). Monitoring accommodative ciliary muscle function using three-dimensional ultrasound. *Graefes Archives of Clinical and Experimental Ophthalmology, 240*(11), 906-912.

Strenk, S. A., Semmlow, J. L., Strenk, L. M., Munoz, P., Gronlund-Jacob, J., & DeMarco, K. J. (1999). Age-related changes in human ciliary muscle and lens: A magnetic resonance imaging study. *Investigative Ophthalmology and Visual Science, 40*(6), 1162-1169.

Strenk, S. A., Strenk, L. M., & Guo, S. (2006). Magnetic resonance imaging of aging, accommodating, phakic, and pseudophakic ciliary muscle diameters. *Journal of Cataract and Refractive Surgery, 32*(11), 1792-1798.

Strenk, S. A., Strenk, L. M., & Guo, S. (2010). Magnetic resonance imaging of the anteroposterior position and thickness of the aging, accommodating, phakic, and pseudophakic ciliary muscle. *Journal of Cataract and Refractive Surgery, 36*(2), 235-241.

Strenk, S. A., Strenk, L. M., & Koretz, J. F. (2005). The mechanism of presbyopia. *Progress in Retinal and Eye Research, 24*(3), 379-393.

Strenk, S. A., Strenk, L. M., & Semmlow, J. L. (2000). High resolution MRI study of circumlental space in the aging eye. *Journal of Refractive Surgery, 16*(5), S659-S660.

Strenk, S. A., Strenk, L. M., Semmlow, J. L., & DeMarco, J. K. (2004). Magnetic resonance imaging study of the effects of age and accommodation on the human lens cross-sectional area. *Investigative Ophthalmology and Visual Science, 45*(2), 539-545.

Tsorbatzoglou, A., Nemeth, G., Szell, N., Biro, Z., & Berta, A. (2007). Anterior segment changes with age and during accommodation measured with partial coherence interferometry. *Journal of Cataract and Refractive Surgery, 33*(9), 1597-1601.

van Alphen, G. W., & Graebel, W. P. (1991). Elasticity of tissues involved in accommodation. *Vision Research, 31*(7-8), 1417-1438.

Vilupuru, A. S., & Glasser, A. (2003). Dynamic accommodative changes in Rhesus monkey eyes assessed with A-scan ultrasound biometry. *Optometry and Vision Science, 80*(5), 383-394.

Weeber, H. A., Eckert, G., Soergel, F., Meyer, C. H., Pechhold, W., & van der Heijde, R. G. (2005). Dynamic mechanical properties of human lenses. *Experimental Eye Research, 80*(3), 425-434.

Wendt, M., Croft, M. A., McDonald, J., Kaufman, P. L., & Glasser, A. (2008). Lens diameter and thickness as a function of age and pharmacologically stimulated accommodation in rhesus monkeys. *Experimental Eye Research, 86*(5), 746-752.